

Chapter 3

Metro Network Simulation

3.1 Photonic Simulation Tools

Simulation of photonic system has become a necessity due to the complex interactions within and between components. Tools have evolved from in-house code, developed for a single purpose, to commercial simulation environments that cover almost all simulation tasks and provide additional functionality to speed the design process, such as the ability to automate the design process and to capture expert knowledge.

Figure 3.1 illustrates the numerous technical challenges of optical systems design arranged on a chart with three axes: optical bandwidth, capacity per channel, and channel density. The volume contains within the axes is the capacity of the transmission system in Gbit/s.

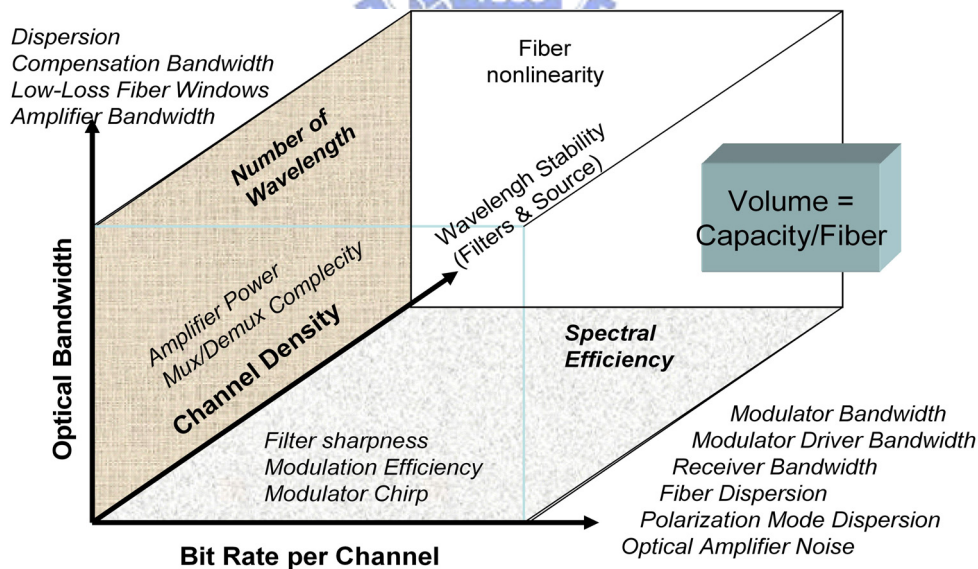


Fig. 3.1 Challenges for optical systems design arranged on three orthogonal axes. The figure comes from the book [3.1].

In 1998, the three popular simulators, BroadNED, GOLD, and OPALS, were merged into one platform using the Ptolemy scheduler for both sample-by-sample

(Sample Mode) data passing and block-by-block (Block Mode) data passing. As shown in Fig. 3.2(a), there is a two-stage iteration process: first, all models are run to calculate their internal states, such as optical fields; second, data is exchanged between adjacent modules to be used in each module's next calculation of its internal state. Around 1996, WDM systems were becoming popular. Figure 3.2(b) shows an interface was operated by passing blocks of data in a "forward" direction, from transmitter to receiver (herein called "Block Mode").

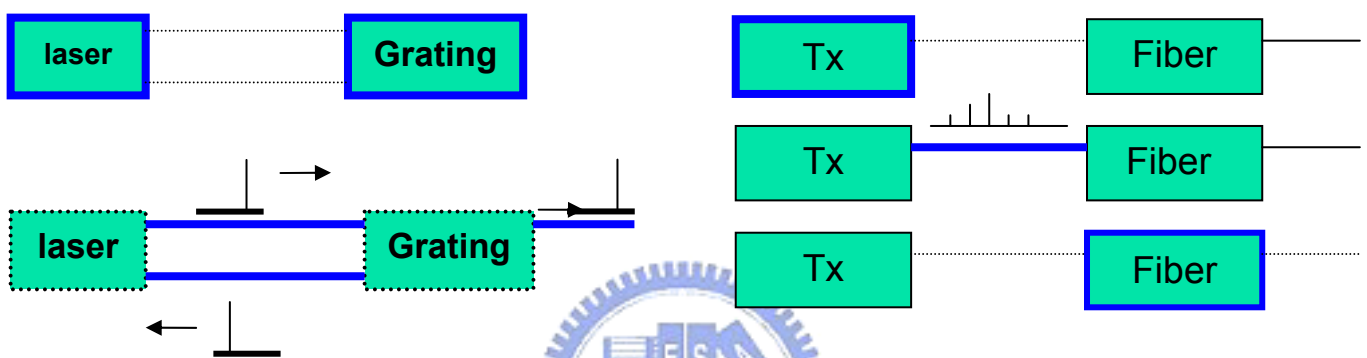


Fig. 3.2(a) Bidirectional simulation algorithm.
(Sample Mode)

Fig. 3.2(b) Passing data uni-directionally simplifies calculations. (Block Mode)

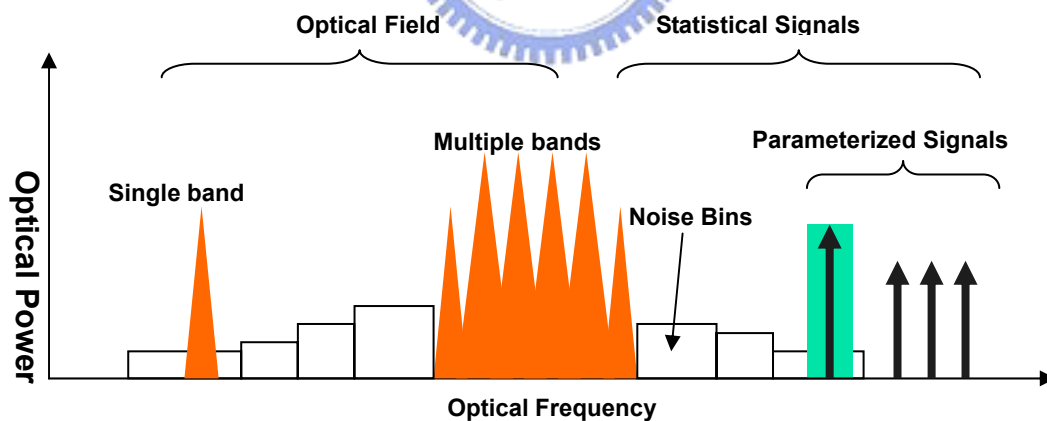


Fig. 3.3 Large channel counts require mixed signal representations to model systems efficiently.

In the WDM system, the VPI usually classifies the simulation data into three categories, sampled signal, parameterized signal, and noise bins, as shown in Fig. 3.3.

For WDM systems, nonlinear effects are of concern, and the simulation of the fiber takes most of the computational effort. Thus it is important to use efficient

methods of computation, such as the split-step Fourier method. But the total Field method may not be the optimum solution for all applications. For this reason, different optical signal representations have been developed, such as mean-field method and semi-analytical methods, etc...

Another important topic is to measure BER. There are two approaches used to BER estimation in simulation. The first is to estimate the noise-induced amplitude distributions based on a significant number (>1024) of bits and a knowledge of the likely form of the noise-induced distribution. This is illustrated in Fig. 3.4(a). The second method is to describe all forms of noise throughout the system with statistical measures, and then propagate these measures throughout the system to the BER estimator, as illustrated in Fig. 3.4(b).

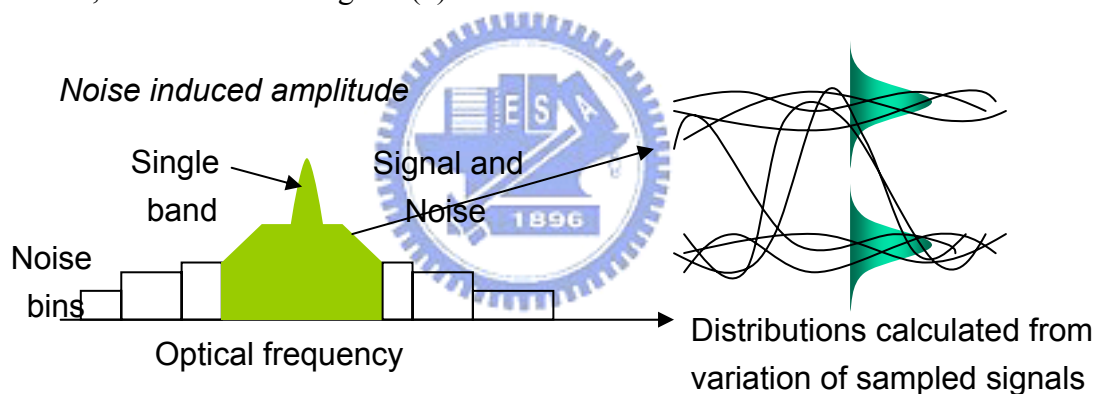


Fig. 3.4(a) BER estimation using curve fitting to estimate noise-induced amplitude distributions.

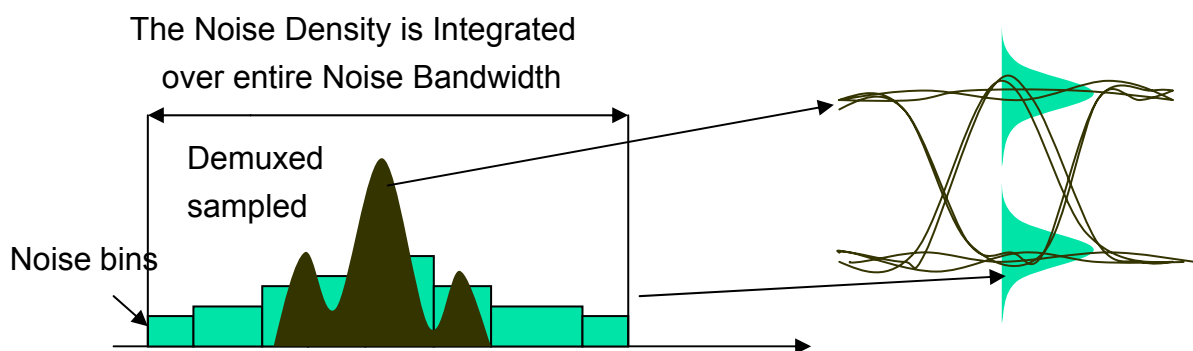


Fig. 3.4(b) BER estimation using deterministic noise passed separately to signal.

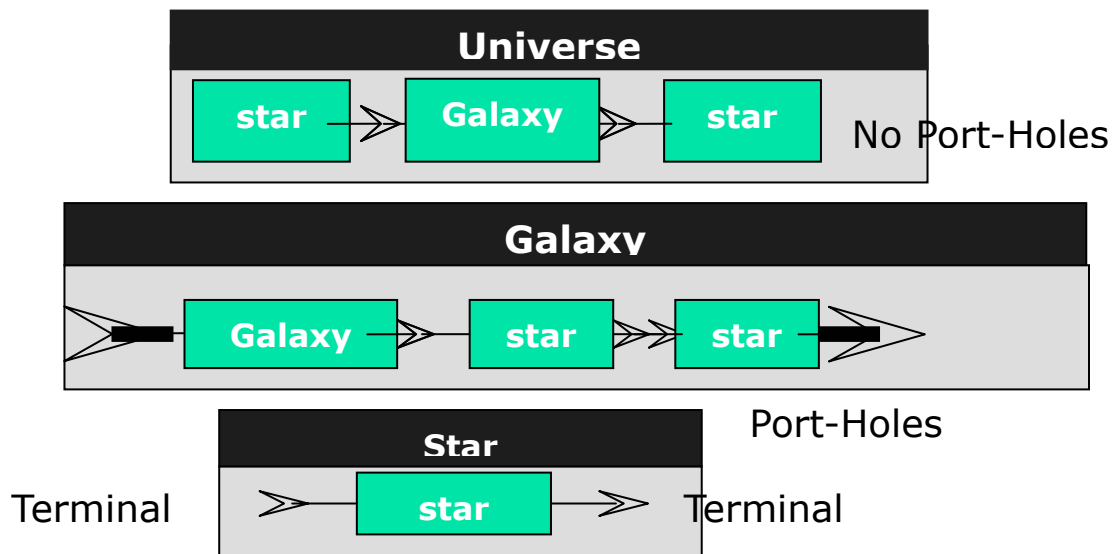


Fig. 3.5 About the hierarchy levels

In the VPItransmissionMaker™, a complete simulation application is called a Universe. A universe consists of a network of interconnected modules that can be stars or galaxies, or both. A Universe can be run as a simulation; galaxies and stars cannot be run, as they require external connections. As shown in Fig. 3.5.

Simulation has advantages, for one, parameters can be set and adjusted with far more certainty than in reality, and measurement errors can be eliminated by removing reflections, unknown losses, and even noise in some cases. Any design process using novel components should include laboratory prototypes, at least until the simulation is verified for these component [3.1]. However, the most important reason for the simulation is to prevent the occurrence of the unworkable experiments, and decrease unnecessary cost and time on experiments.

3.2 Creating Two Types of Interleaver pairs in VPI

By using the co-simulation interface in VPItransmissionMaker™, I created a galaxy containing the required input and output ports. At each port, there is an engine to exchange the data form VPI to matlab or matlab to VPI. A single co-simulation module drives simulation in the target environment (matlab).

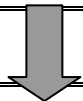
3.2.1 The Transformation of Data Structures between VPI and Matlab

Optical signals are represented using structures as shown in Table 3.1. The top level structure contains some general signal information starting with the time and frequency grid spacing already mentioned (dt and df). The timestamp (start time) and duration of signal (t0 and T) and the upper and lower frequency limits (f1 and f0). Note that these time and frequency values are given as integer multiples of the respective grid spacing. For signal with periodic boundary conditions, the timestamp has well-defined meaning since the block of data represents one period of a waveform that extends in principle over all time. In this case, the time stamp will typically be zero.

There are three arrays, sampled frequency bands, parameterized signals, and noise bins, in the simulation. Each of these signal representations is stored in a separate structure located in the respective array. The contents of these structures are also displayed in Table 3.1[3.2].

The data structure of the interleaver model consists of three important parameters, amplitude, phase, and frequency. Therefore, we just care about the sample band in Table 3.1, in which the entries of Ex and Ey can not be used in the program. And we also don't care about any parameter related to polarization, such as azimuth (azi) and ellipticity (ell). The reason is that there is not any polarization problem in the interleaver device.

Optical signal representation (Block Mode)		
structure entry	type	Description
type: 'osignal'	string	signal type: optical signal
dt	float	time grid spacing (seconds)
df	float	frequency grid spacing (Hz). $df=1/TimeWindow$
t0	int	time stamp (start time) of signal (grid points)
T	int	duration of signal (grid points)
f0	int	lower frequency limit (grid points)
f1	int	upper frequency limit (grid points)
noise	array	contains Noise Bins if present
channels	array	contains Parameterized Signals if present
<i>bands</i>	array	contains sampled bands if present



Sampled Band		
structure entry	type	Description
type: 'oband'	string	signal type: sampled signal
f0	int	lower frequency limit (grid points)
f1	int	upper frequency limit (grid points)
azi	float	azimuth of polarization ellipse in degrees
ell	float	ellipticity of polarization ellipse in degrees
E	complex array	optical field in case of fully polarized signal
Ex	complex array	x-polarization of optical field
Ey	complex array	y-polarization of optical field

Table 3.1 Representations of optical signals (Block Mode)

3.2.2 Implementing an Interleaver Pair by Using Matlab

In the real world, the interleaver device is bi-directional, but there is a single direction in the VPI. So I must distinguish them into multiplexer and de-multiplexer. The structure is shown in Fig. 3.6. The intrinsic insertion loss is needed to set 2.9dB by the attenuator. The Matlab code filters the input data with a constant polarization, copes with it by a single array of complex samples, and uses one approach to quantize its frequency. The total bandwidth of the signal is stored as an integer bw representing the number of frequency grid steps. The center frequency of the band (in Hz) is computed as the initial value of the optical frequency f ($f = x.df * (x.bands\{band\}.f0 + bw/2)$). Filtering is performed in the frequency domain by multiplying each component of the discrete Fourier transform of the sampled band by the interleaver transfer function. The standard layout of the array containing the FFT result consists of the samples corresponding to all frequencies from the center frequency up to the maximum frequency first, followed by the samples corresponding to the minimum frequency up to the center frequency. Thus, at the half-way point, the physical frequency reaches the maximum frequency, and must be reduced to the minimum frequency by subtracting the bandwidth.

The dispersion free combination by cascading type-A and type-B interleaver is called type-AB, the other one without dispersion compensation by cascading type-A and type-A is called type-AA.

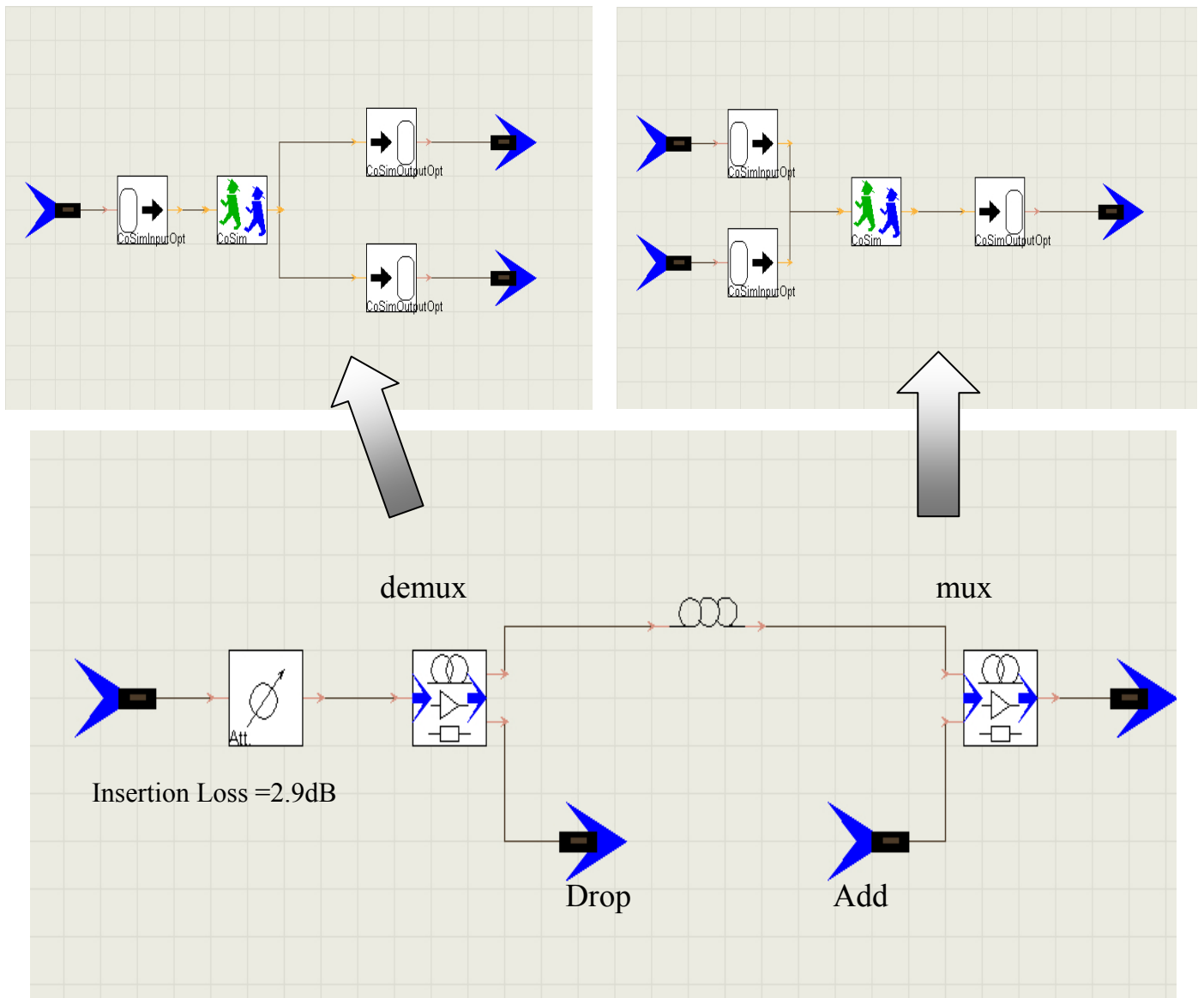


Fig. 3.6 Co-simulation galaxy for the Matlab interleaver pair (Add/Drop Node)

3.3 Simulation of the Metro network

3.3.1 The channel numbering

My model is a ideal model without considering the variation of the fraction index of the birefringent crystal and temperature compensation, so it is easy to design for matching the ITU channels (Table.2).

“Odd” Port		“Even” Port	
Passband		Passband	
Channel	CWL(nm)	Channel	CWL(nm)
9530	1535.034	9540	1534.248
9510	1536.607	9520	1535.820
9490	1538.184	9500	1537.396
9470	1539.764	9480	1538.974
9450	1541.348	9460	1540.556
9430	1542.934	9440	1542.141
9410	1544.524	9420	1543.729
9390	1546.117	9400	1545.320
9330	1550.916	9340	1550.115
9310	1552.523	9320	1551.719
9290	1554.132	9300	1553.327
9270	1555.745	9280	1554.938
9250	1557.362	9260	1556.553
9230	1558.981	9240	1558.171
9210	1560.604	9220	1559.793
9190	1562.231	9200	1561.417

Table 3.2 Center Wavelength Designations for pass band for each through path

3.3.2 The comparison between cascading 24 type-AB and type-AA interleaver pairs

The transmitters, receivers and add/drop node (A/D N) block diagrams are shown in Fig. 3.7. The model consists of alternating spans of a type-AB or type-AA interleaver pair and an ideal optical amplifier (noise figure=5). Each system was set

by cascading 24 type-AB or type-AA interleaver pairs. Single channel spacing is 100 GHz for 10, 20 and 40 Gbit/s signals. A 128-bit pattern is encoded using either NRZ or RZ modulation (RZ duty cycle = 50%). At receiver, the optical bandpass filters are two and four times of bit rate (2R and 4R), respectively, for NRZ and RZ modulation formats. Then, the signal is electrically low-pass filtered with filter bandwidth 1.5R (f_{3dB}). For 40Gbit/s RZ system, the optical bandpass filter is 2.5R and the electrical filter bandwidth is also 1.5R. System performance is evaluated by measuring the channel Q factor.

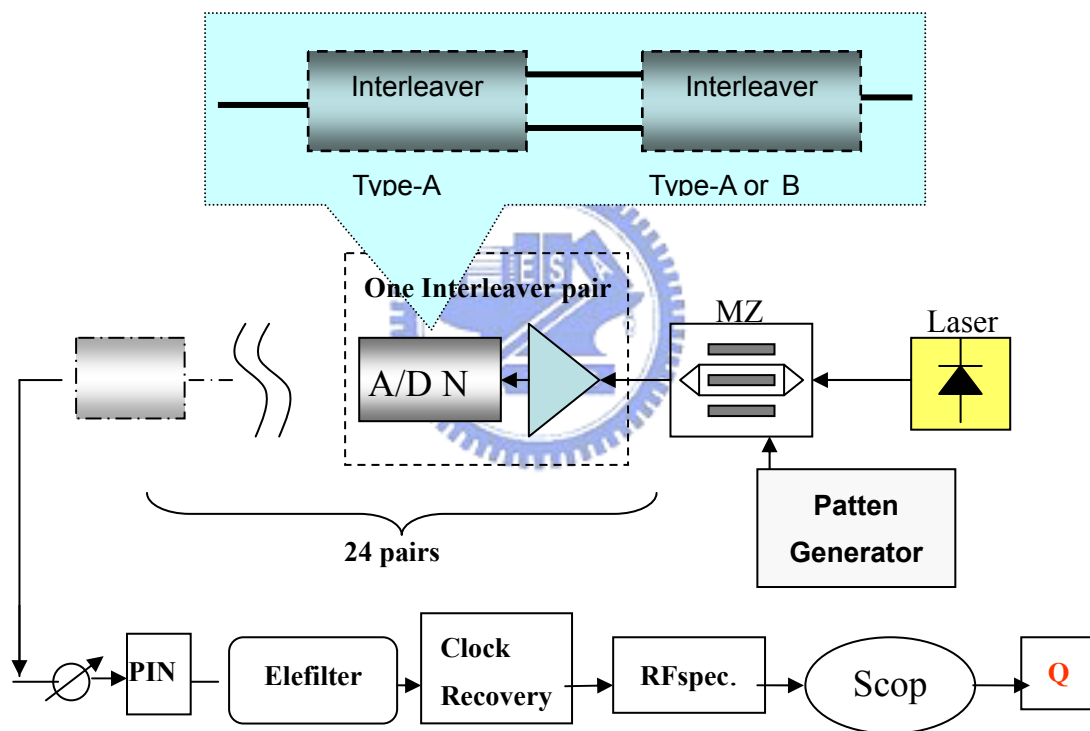


Fig. 3.7 Simulation of configuration using RZ and NRZ modulations with 24 interleaver pairs.

In fig. 3.8, a convenient relationship to bear in mind is that BER of 10^{-12} requires a Q factor of 16.9dB ($20 \cdot \log_{10}(q)$). In a 10-Gbit/s RZ system, compare to the line of $Q=7$ (16.9 dB), the combination of type-AA or type-AB had more 14 dB margin. And the two kinds of combinations both had a good performance even passing

through 24 interleaver pairs. In a 20Gbit/s system, the margins of the two combinations are decreasing following with the number of the interleaver pairs. Although the Q-factor of type-AA becomes smaller quickly during the preceding 12 pairs, the type-AB already had a good performance after 24 pairs. In the 40-Gbit/s system, the Q-factor of the type-AB is degrading form the 12th pair to the 24th pair. Moreover, the Q-factors of the type-AA are almost lower then 16.9 dB just at the 6th pair, and decrease to 10dB at the 12th pair. Figure 3.8 shows received eye diagrams for two combinations of the interleaver in 10, 20 and 40 Gbit/s. The eye closure is due to accumulated dispersion in type-AA and the pass band ripple of the interleaver transfer function in both two combinations. Figure 3.9 shows the optical signal to noise ratio (OSNR) for the same situation, and the degrading of OSNR results from the noise figure of the ideal amplifiers.

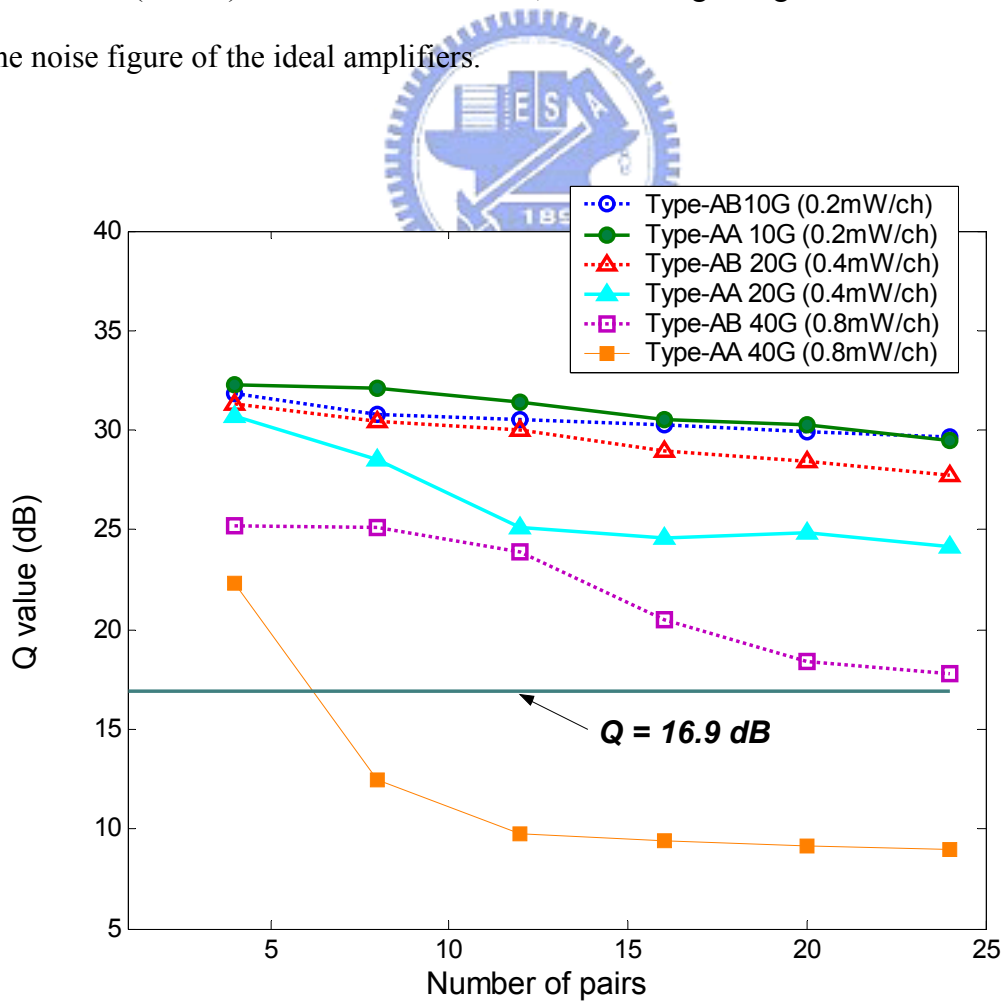


Fig. 3.8 Q-factor of the RZ system with the type-AB and type-AA interleaver pairs

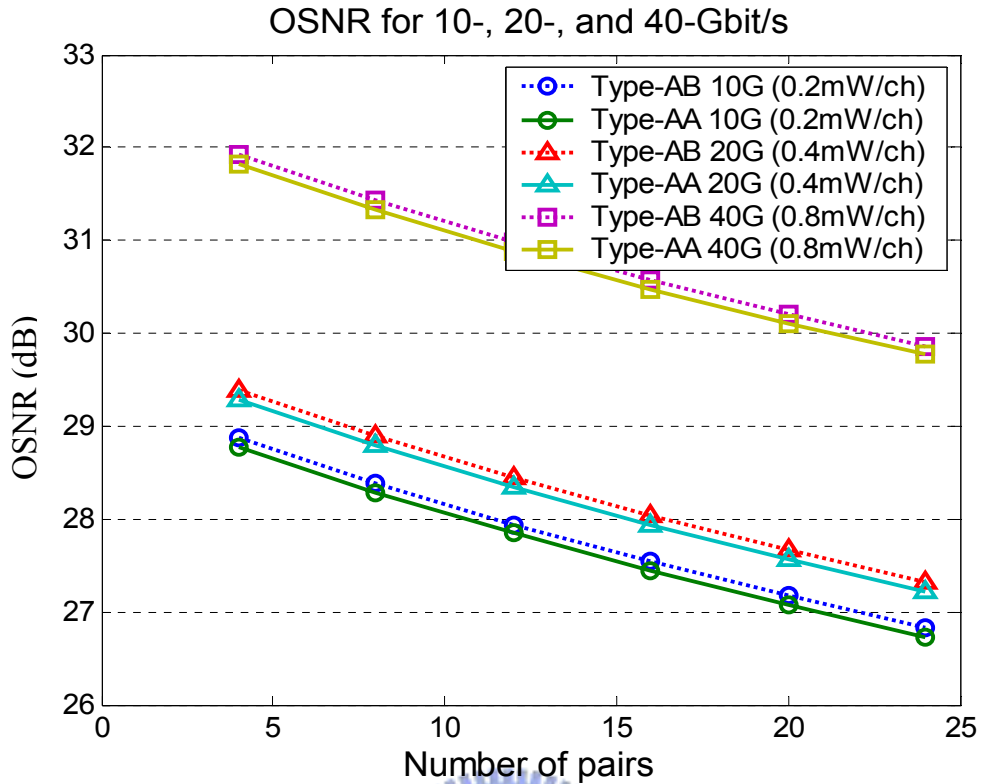
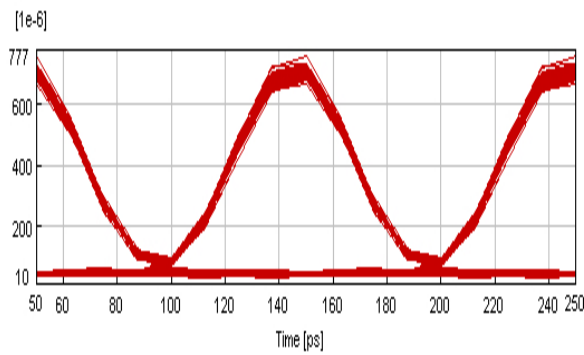
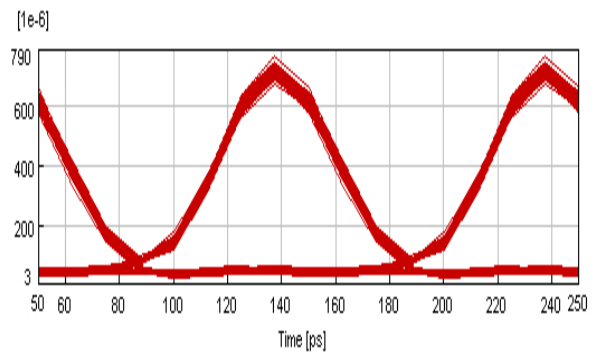


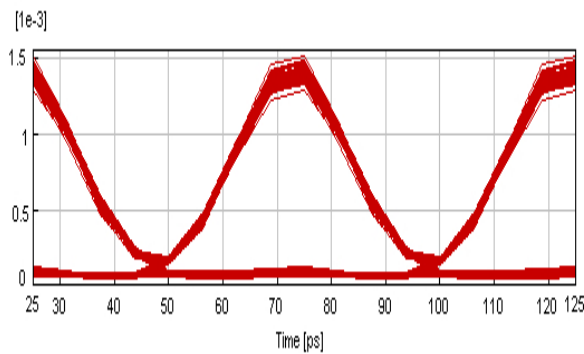
Fig. 3.9 The OSNR of the RZ system with the type-AB and type-AA interleaver pairs



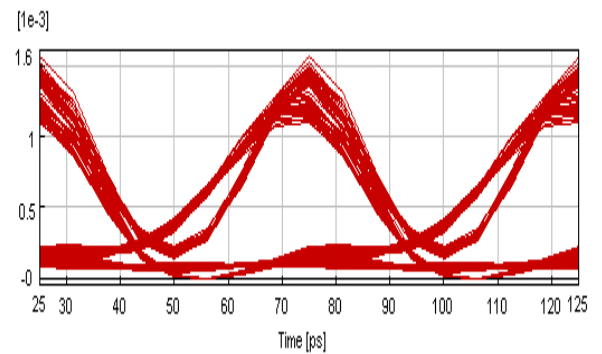
Type-AB RZ 10-Gbit/s pass 24 pairs



Type-AA RZ 10-Gbit/s pass 24 pairs



Type-AB RZ 20-Gbit/s pass 24 pairs



Type-AA RZ 20-Gbit/s pass 24 pairs

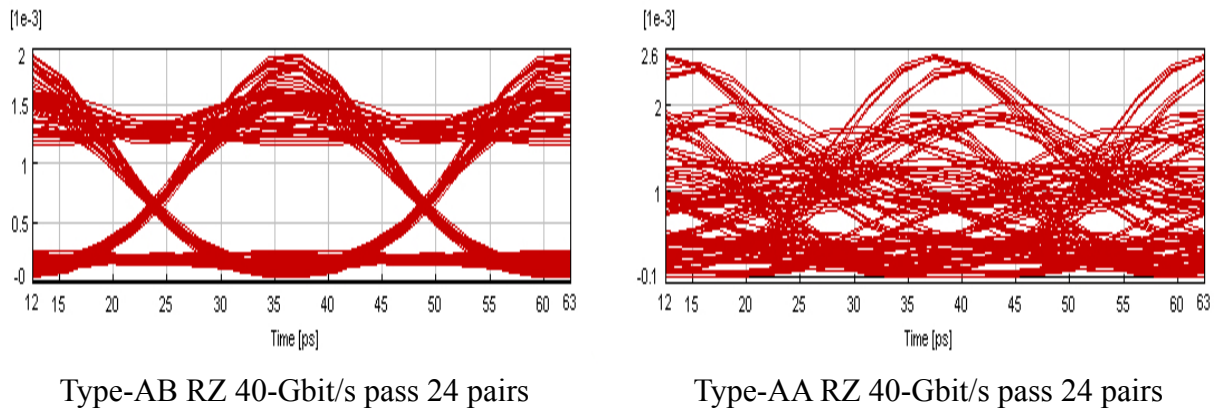


Fig.3.10 Eye diagrams for 10, 20 and 40 Gbit/s

About the degrading effect caused by the dispersion effect during the 24 type-AA interleaver pairs, the key point is the difference of delay in the first harmonic range. The delay differences in the first harmonic are shown in Fig. 3.11(a)-(c), respectively, for 10-, 20-, and 40-Gbit/s RZ systems. In Fig. 3.11(a), the maximum difference of delay is about 3.0ps in the the first harmonic of double side band at 10Gbit/s for RZ system. It is too difficult to degrade the performance in this system, because the bit time of 10-Gbit/s is 100ps. In Fig. 3.11(b), the maximum difference of delay is about 10.5ps in the first harmonic range. Compare to the bit time of 20-Gbit/s (50ps), the difference is not small enough to keep the good performance. Fortunately, the frequency range of the high delay difference just have few percentage in the first harmonic rang. However, in the 40-Gbit/s system, the maximum of delay difference is about 35ps, and the frequency range occupies the 20% in the first harmonic range [Fig. 3.11(c)]. Besides for the dispersion effect, the bandwidth of optical filter (100 GHz) let the signal of the 40-Gbit/s loss too much power.

It is the same principle to analyze the NRZ system about the delay difference of the two types. We also can generally explain the phenomenon in Fig. 3.15 by Fig. 3.12. The bandwidth of the radio frequency (RF) spectrum for RZ signal is two

times of NRZ signal. Therefore, the performance, Q-factor, eye closure, optical signal to noise ratio (OSNR), or bit error rate (BER), of the 40-Gbit/s NRZ system for should be obviously better than the 40Gb/s RZ system. But actually, the NRZ modulation also suffers from the higher nonlinearity than the RZ modulation; for this reason, the two modulation types have the same performance, as shown in section 3.2.

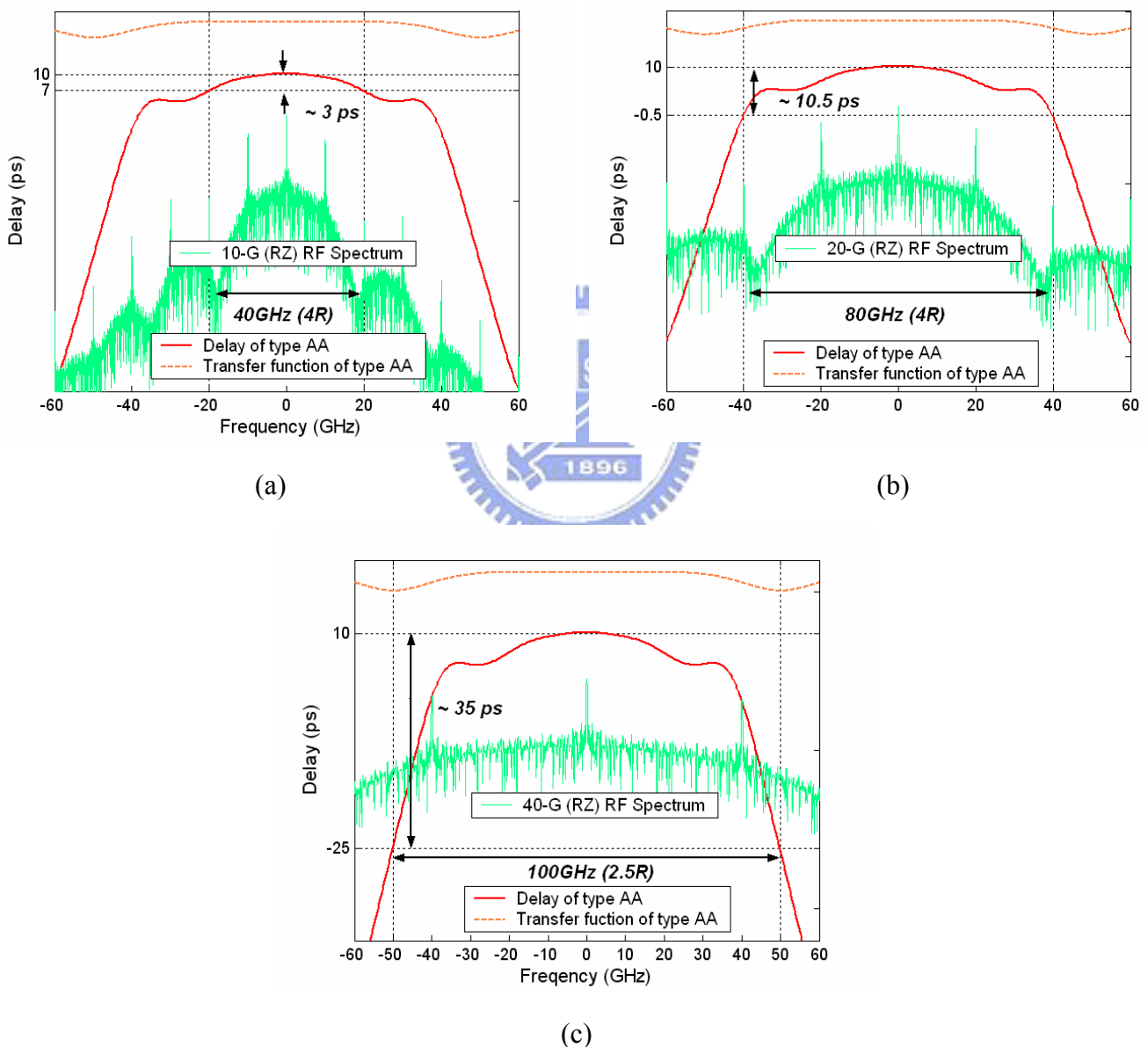


Fig. 3.11. The delay and the transfer function of type AA at (a) 10 Gbit/s, (b) 20 Gbit/s, and (c) 40 Gbit/s. (RZ format)

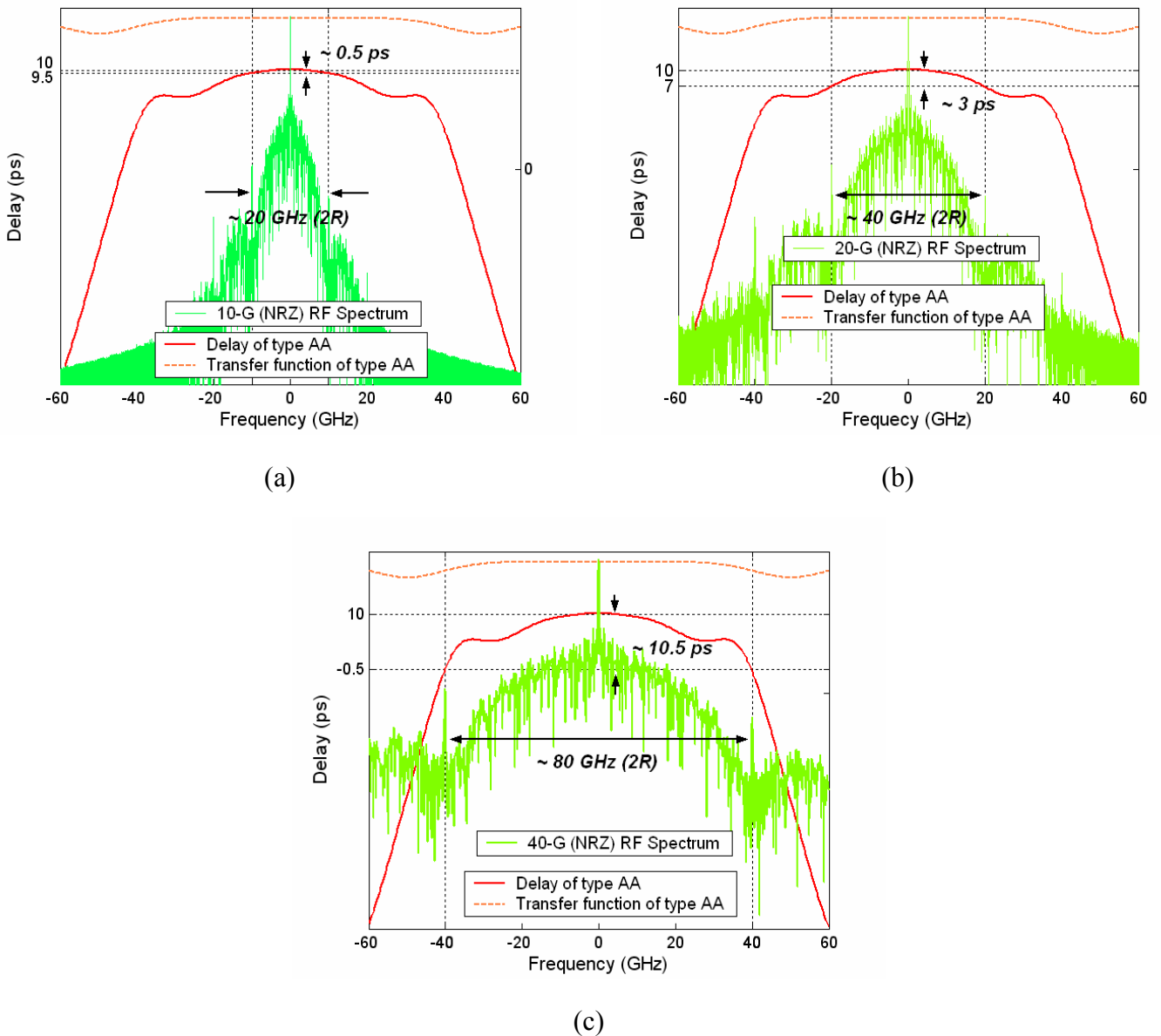


Fig. 3.12 The delay and the transfer function of type AA at (a) 10 Gbit/s, (b) 20 Gbit/s, and (c) 40 Gbit/s. (NRZ format)

3.2 Point-to-point simulation for metro add/drop network

Figure 3.13 shows the simulation setup by VPI transmission Maker. My model consists of alternating fiber spans of 50 km of SMF ($D = +17$ ps/nm/km, dispersion slope = $+0.08$ ps/nm²/km) and 10 km of DCF ($D = -85$ ps/nm/km, dispersion slope = -0.4 ps/nm²/km), followed by an ideal optical amplifier (noise figure = 5) and an A/D node (Insertion loss = 2.9 dB). *Note that this model is a perfect Fourier dispersion and dispersion slope compensation system in each fiber span.* WDM channel spacing

is 100 GHz for 10, 20 and 40 Gbit/s signals and the thirty-two 100-GHz spaced channels confirm with the channel numbers in Table 3.2. A 128-bit pattern is encoded using either NRZ or RZ modulation (RZ duty cycle = 50%) with the extinction ratio of 12dB, and the propagation of the combined optical field is simulated by nonlinear Schrödinger equation [3.3]. At the receiver, each WDM channel is optically demultiplexed with a bandpass filter of 2R and 4R, respectively, for NRZ and RZ modulation formats. Especially for the 40 Gbit/s system, the optical filter bandwidth is 2.5R (spectral efficiency = 0.4). Each demultiplexed channel is then electrically low-pass filtered with a filter bandwidth 0.8R. The system performance evaluation is base upon the Q-factor (dB) and dQ (Q penalty) of each channel including shot noise and thermal noise (10^{-8} mW).

The global parameter “SampleRates” was set to 16*bit rate. And the sample rates of the individual transmitters must be greater than the WDM channel spacing, because the WDM channels will be merged into a single sampled band (SFB). SFB gives the most general case, including the modeling of Four-Wave Mixing. However, the multiple frequency bands (MFB) cannot represent crosstalk between channels due to four-wave mixing [3.4]. In addition, the noise bins always represent spectral noise outside the sampled bands, they can used to combine noise within the range of the sampled bands by setting the global parameter InBandNoiseBins = OFF. The combination propagation of signals and noise is useful for “noise-induced amplitude” estimation of bit error ratio, as discussed in “BER estimation” in Fig. 3.4(a).

According the setup of WDM system, I compare the two combinations of the interleaver pairs (type-AA and type-AB) for 10-, 20-, or 40-Gbit/s signal coded by NRZ or RZ format.

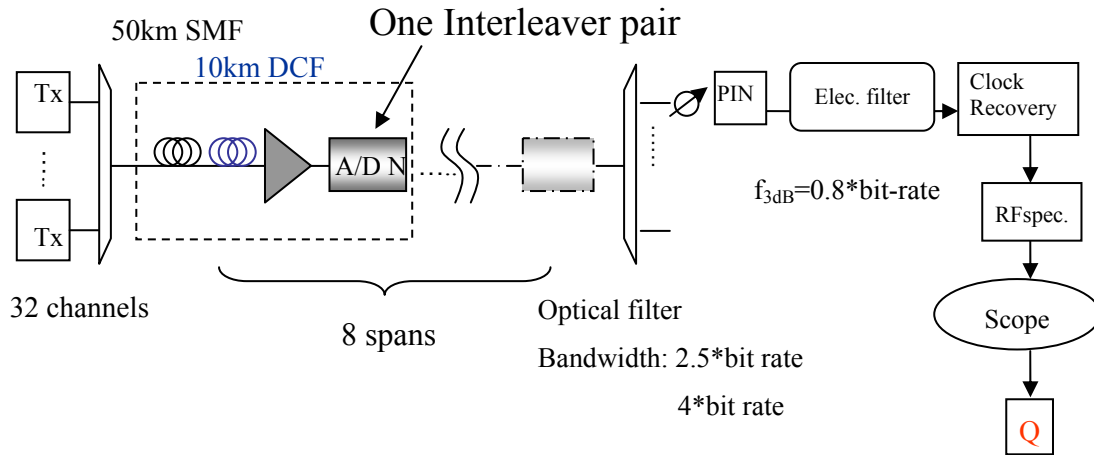


Fig. 3.13 Simulated diagram of 32 channels metro WDM system

3.2.1 NRZ format

Figure 3.14 shows the received eye diagrams for the worst channel. The eye diagrams shown are from up to down: 10-, 20-, and 40-Gbit/s system. Besides for the eye closure due to accumulated noise, the accumulated dispersion by the type-AA interleave pairs is also one of key parameter to make the eye close, especially in 40-Gbit/s system.

Figure 3.15 shows the received spectrum after the fiber of 424 km, 8 ADNs, and 8 ideal amplifier (NF = 5). The average received OSNRs of all situations in 10 GHz resolution bandwidth (RBW) were about 30 dB.

The system performances are shown in Fig. 3.16 (a)-(c), respectively, for 10-, 20-, and 40-Gbit/s signals. In the 10-Gbit/s system, the average Q-factor of all channels in the type-AB and type-AA was respectively 20.4dB and 20.3dB; and the worst Q-factor in the type-AB system was about 18.8dB. Compared to the line of Q=16.9dB the two combinations had more than 3.4dB margin. Then, in the 20-Gbit/s system, the average Q-factor of the type-AB was down to 20.3dB and the margin also keeps in 3.4dB. But the margin of the type-AA degraded to about 2.8dB. Finally, the average Q-factor in the type-AA was no longer upper than 16.9dB, and decreased to 12.1dB. By contrast, the type-AB obviously exceeds the type-AA in the average

Q-factor of about 5.2dB in the 40-Gbit/s system and the margin compared to $Q=16.9\text{dB}$ in the type-AB system was almost left over 0.4dB. Figure 3.15(c) shows the type-AB interleaver pairs can satisfy the strict requirements in the 40-Gbit/s DWDM metro network.

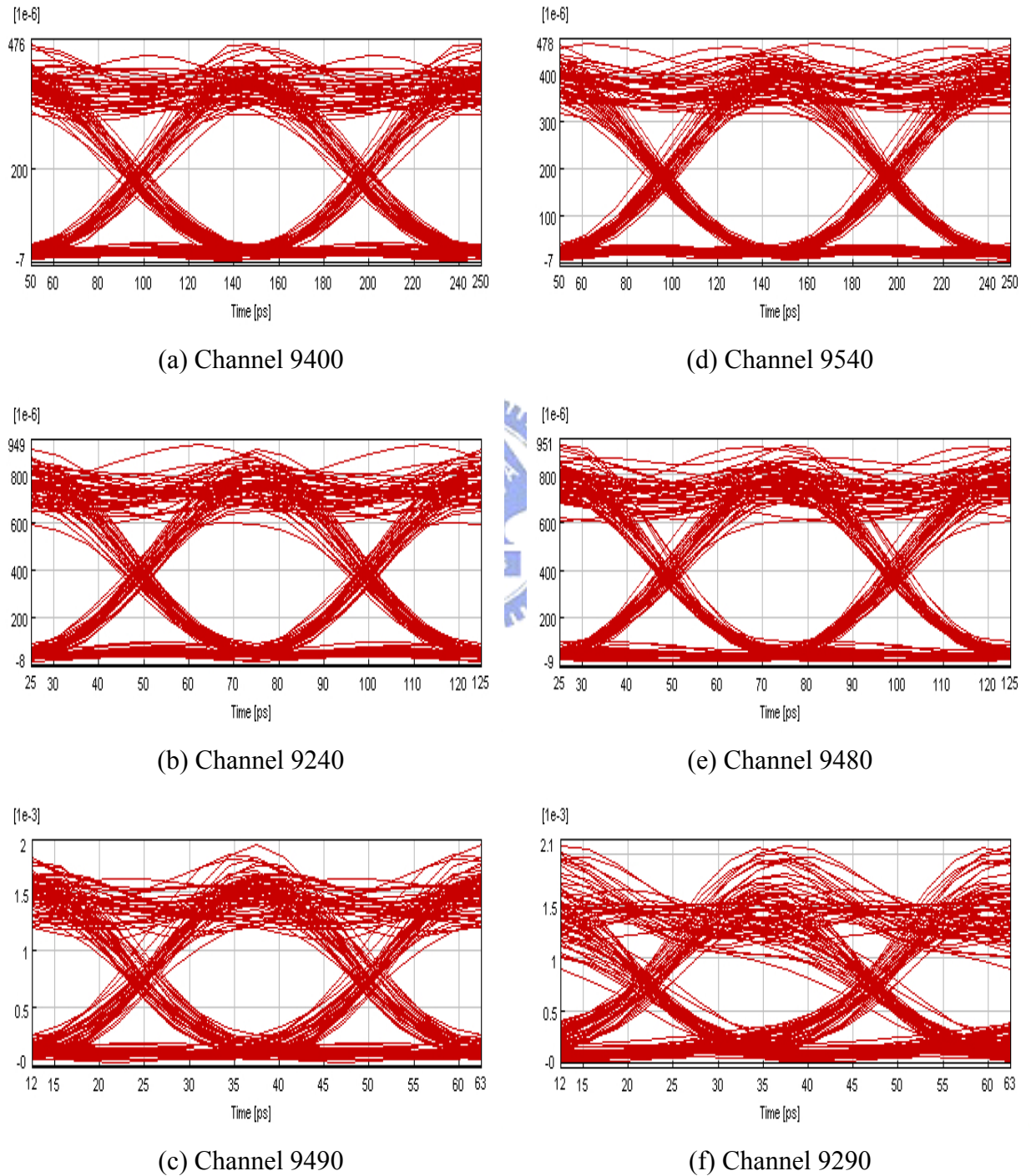
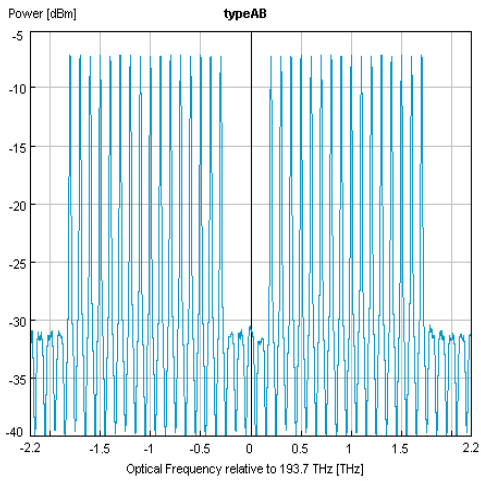
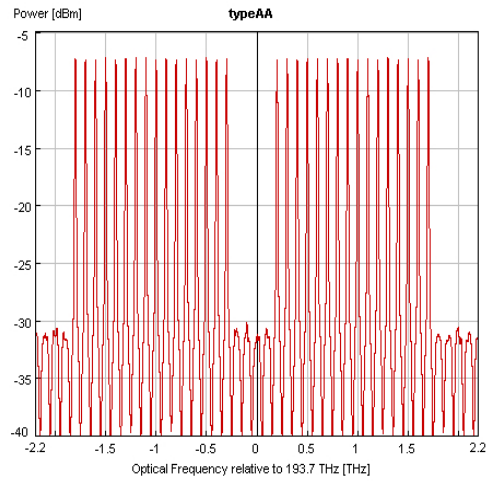


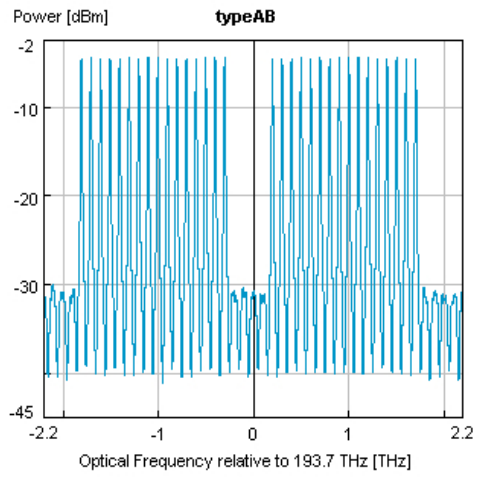
Fig. 3.14 The eye diagrams of the worst channel for 10-, 20-, and 40-Gbit/s NRZ signals. (a)-(c) for type-AB and (d)-(f) for type-AA



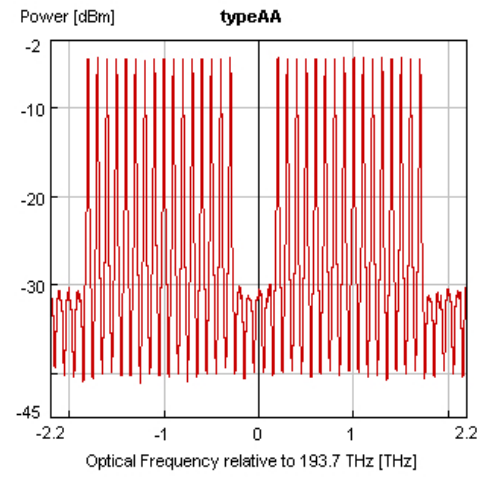
(a) OSA for type AB (10G NRZ)



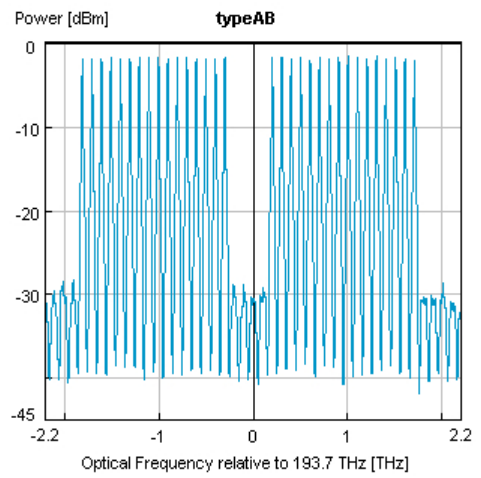
(d) OSA for type AA (10G NRZ)



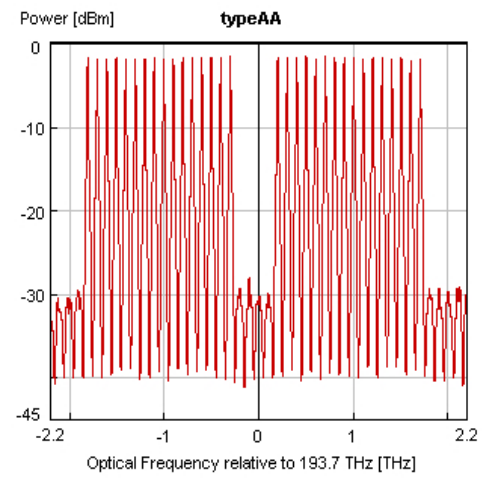
(b) OSA for type AB (20G NRZ)



(e) OSA for type AA (20G NRZ)

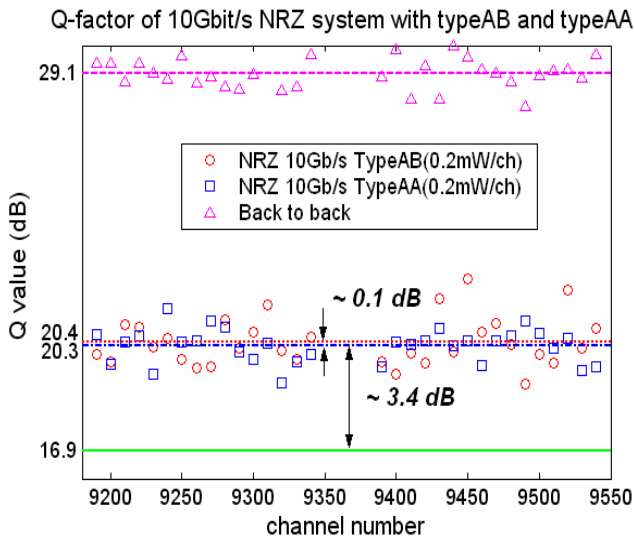


(c) OSA for type AB (40G NRZ)

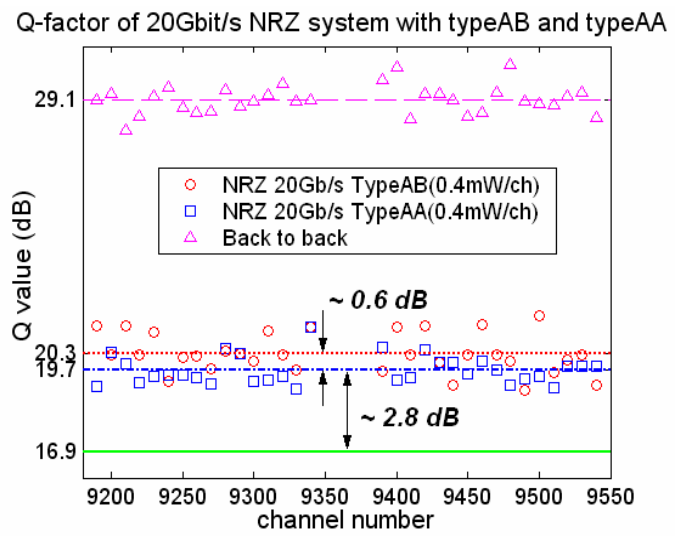


(f) OSA for type AA (40G NRZ)

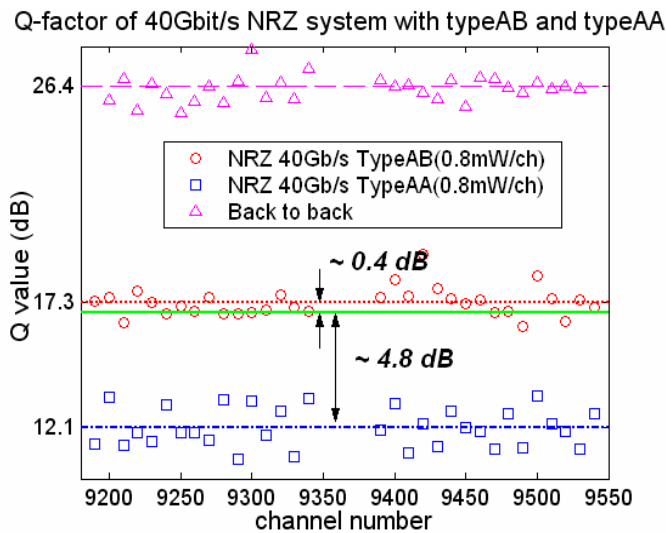
Fig. 3.15 The received optical spectrums in 10GHz resolution bandwidth (RBW).



(a) 10-Gbit/s



(b) 20-Gbit/s



(c) 40-Gbit/s

Fig. 3.16 The Q-factor (dB) plots of type-AA and type-AB at (a) 10 Gbit/s, (b) 20 Gbit/s, and (c) 40 Gbit/s.

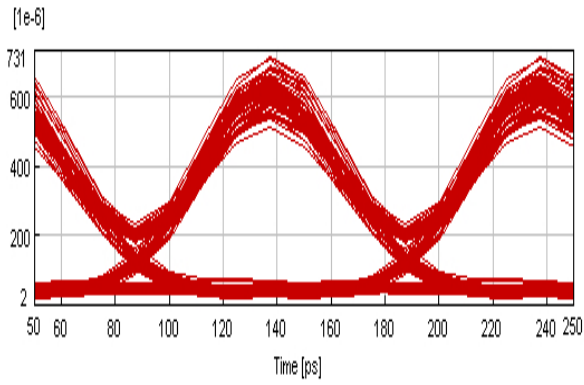
3.2.2 RZ format

Figure 3.17 shows the received eye diagrams of the worst channel. The eye diagrams shown are from up to down: 10-, 20-, and 40-Gbit/s system. Besides for the eye closure due to accumulated noise and the accumulated dispersion by the type-AA interleaver pairs, the overlapping power from the neighboring channels becomes the noise in the local channel (called interchannel crosstalk) to make the eye

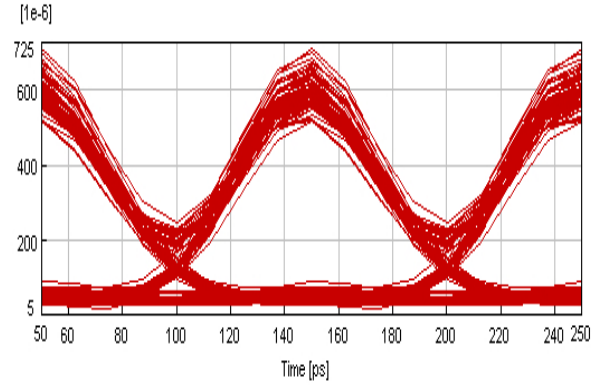
close. Especially in 40-Gbit/s system, the spectral efficiency of 0.4 causes the serious out-of-band crosstalk, and the eye closure depends on the power of the neighboring channels. The crosstalk was combined with the accumulated dispersion from the type-AA system, the eye of the 40-Gbit/s system close perfectly as shown in Fig. 3.17(f).

Figure 3.18 shows the received spectrum after the fiber of 424 km, 8 ADNs, and 8 ideal amplifier (NF = 5). The average received OSNRs of all channels of the 10-, 20-Gbit/s system in 10 GHz resolution bandwidth (RBW) were about 30 dB. Because of the out-of-band crosstalk, the signal power loss larger power and the extra noise power comes from the neighboring channels, the average received OSNR of all channels of the 40-Gbit/s system is decreased to 25dB as shown in Fig. 3.18(f).

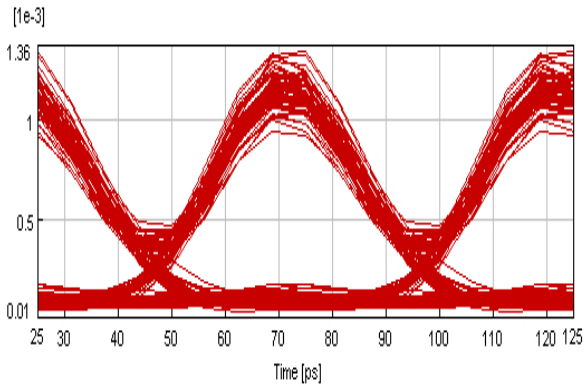
The system performances are shown in Fig. 3.19 (a)-(c), respectively, for 10-, 20-, and 40-Gbit/s. In the 10-Gbit/s system, the average Q-factors of all channels in the type-AA and type-AB system were 21.1dB and 20.8 dB, respectively, and the worst Q-factor of two combinations was about 18.5dB. Compared to the line of Q=16.9dB the average Q-factors had more then 3.9dB margin. Then, in the 20-Gbit/s system, the average Q-factor of the type-AB was down to 20.7dB and it also keeps in 3.8dB margin. The type-AA system also had about 3.6dB margin. Finally, the average Q-factor in the type-AA system was no longer upper than 16.9dB, and decreased to 11.5dB. By contrast, the type-AB obviously exceeds the type-AA in the average Q-factor of about 4.2dB in the 40-Gbit/s system and the Q-factor of the type-AB system was less then Q=16.9dB about 1.1dB. The fig. 3.18(c) shows the type-AB can still be grudgingly used in the 40-Gbit/s system.



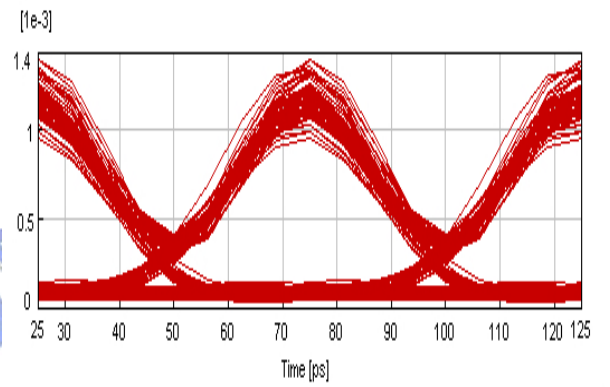
(a) Channel 9440



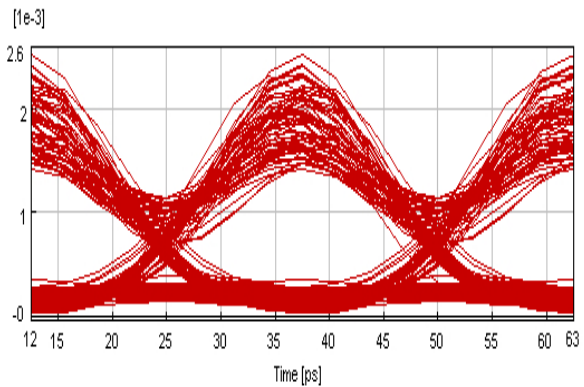
(d) Channel 9520



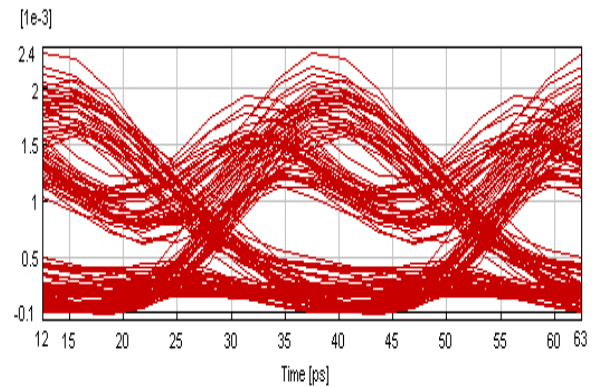
(b) Channel 9250



(e) Channel 9410

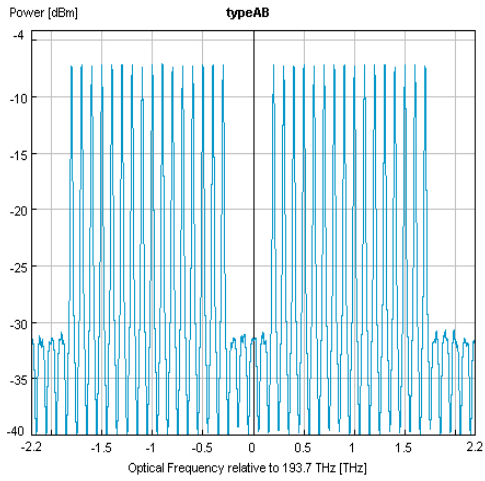


(c) Channel 9200

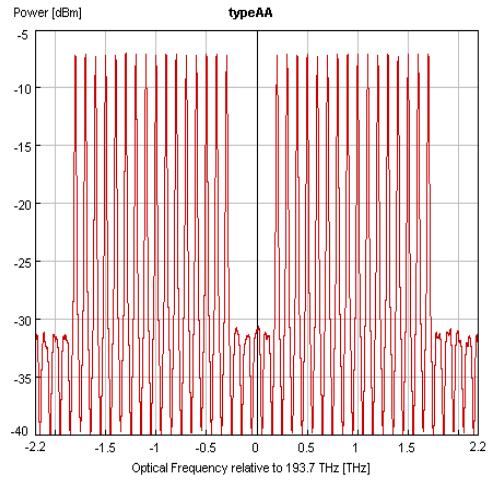


(f) Channel 9200

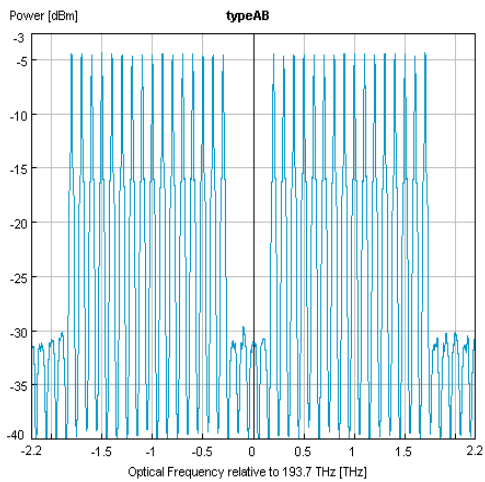
Fig. 3.17 The eye diagrams of the worst channel for 10-, 20-, and 40-Gbit/s RZ signals. (a)-(c) for type-AB and (d)-(f) for type-AA



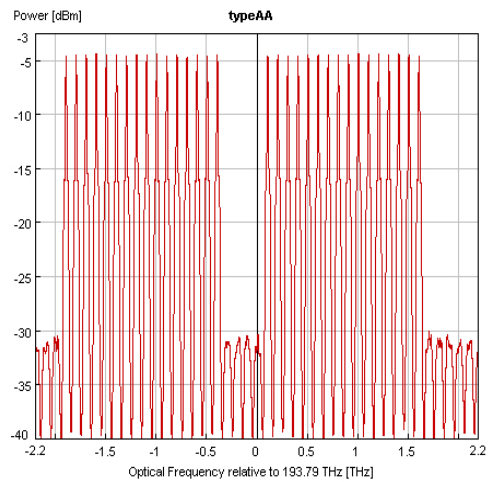
(a) OSA for type AB (10G RZ)



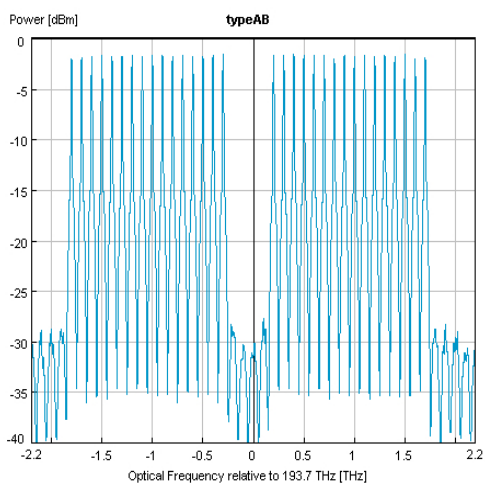
(d) OSA for type AA (10G RZ)



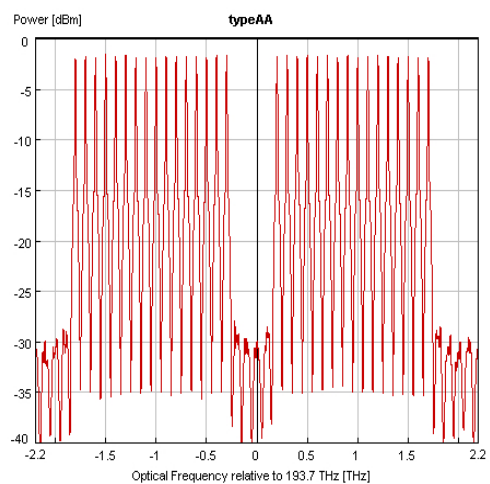
(b) OSA for type AB (20G RZ)



(e) OSA for type AA (20G RZ)



(c) OSA for type AB (40G RZ)



(f) OSA for type AA (40G RZ)

Fig. 3.18 The received optical spectrums in 10 GHz resolution bandwidth.

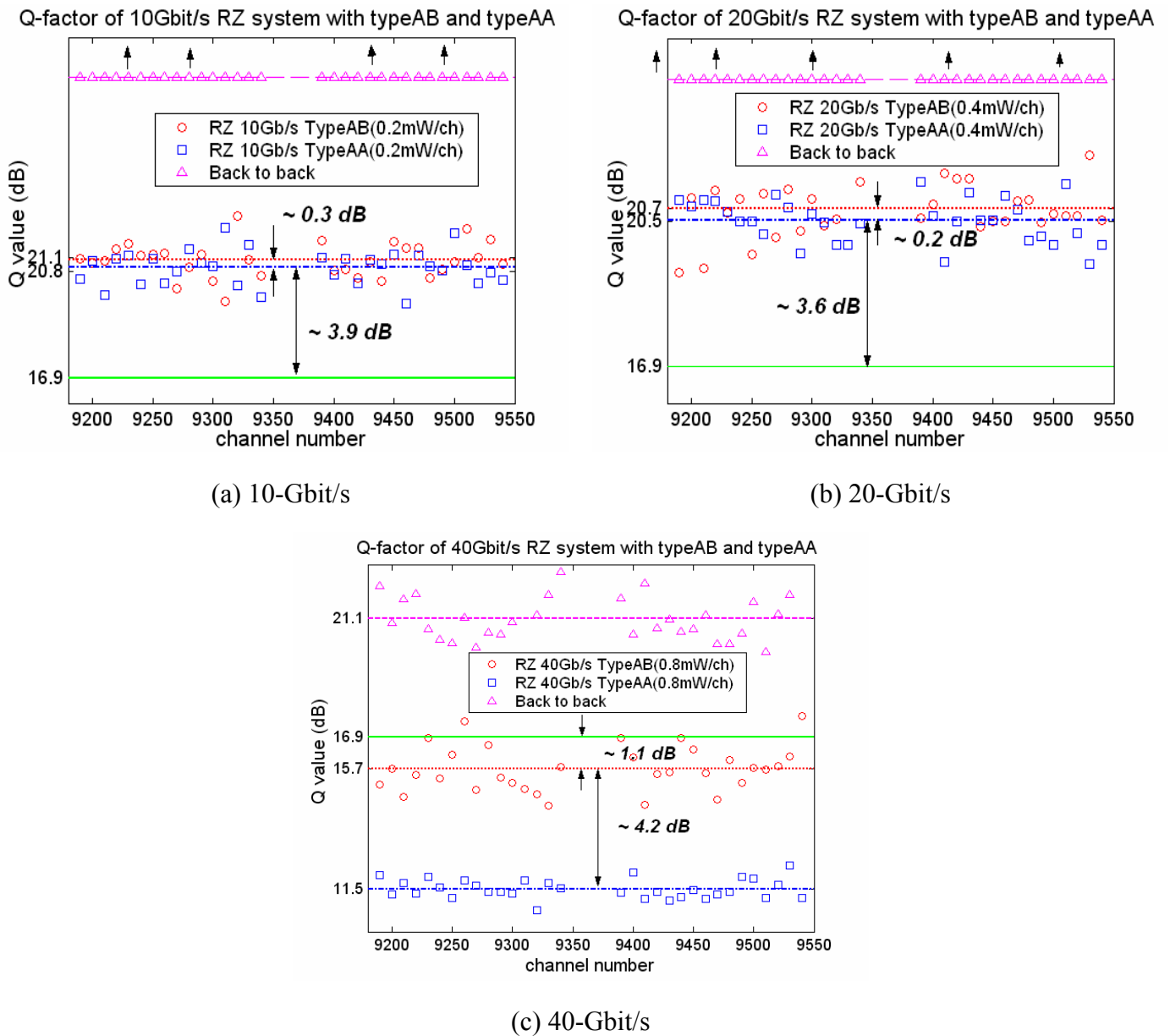


Fig. 3.19 The Q-factor (dB) plots of type-AA and type-AB at (a) 10 Gbit/s, (b) 20 Gbit/s, and (c) 40 Gbit/s.

References

- [3.1] Ivan Kaminow, Tingye Li, *Optical Fiber Telecommunications IVB, systems and impairments*, Academic press, AP, chapter 12.
- [3.2] VPI, *User's Manual*, chapter 12.
- [3.3] VPI, *Photonic Moudules Reference Manual, Vol. I*, pp. 8-1.
- [3.4] VPI, *WDM User's Manual*, chapter 1, pp. 15.